Characteristics of Ru etching using ICP and helicon O_2/Cl_2 plasmas

Hyoun Woo Kim*

School of Materials Science and Engineering, Inha University, Incheon 402-751, Republic of Korea

Available online 24 August 2004

Abstract

We have investigated and compared the characteristics of Ru etching by employing O_2/Cl_2 inductively coupled plasma (ICP) and helicon plasma. We have studied the variation of Ru etch rate and the Ru to SiO_2 etch selectivity with varying the gas flow ratio, the bias power, and the total gas flow rate. With optimizing the process for two different plasma sources, we have obtained higher etch rate of Ru electrode by using ICP, compared to by using helicon plasma. We demonstrated the etching slope of greater than $85°$ in terms of real pattern, using ICP. X-ray photoelectron spectroscopy (XPS) revealed that the Ru surface etched using ICP contained less amount of O element than using helicon plasma.
© 2004 Elsevier B.V. All rights reserved.

Keywords: Etching; Ruthenium; Plasma processing and deposition

1. Introduction

As dimensions of dynamic random access memory (DRAM) devices are become smaller, high dielectric materials such as barium strontium titanate (BST) and tantalum pentoxide (Ta_2O_5), need to be used for the fabrication of capacitor structure [1,2].

Although platinum (Pt) has commonly been utilized as an electrode material, Pt has a difficulty in patterning and thus in forming a bottom electrode. Several research groups have reported that obtaining a sufficient etch selectivity of Pt to the mask material was extremely difficult [3–6]. On the other hand, ruthenium (Ru) is expected to be patterned by chemical etching because volatile RuO_4 can be generated from RuO_2, which is an intermediate phase of the Ru etching reaction [7–9].

However, to our knowledge, comparison of Ru etching behavior in two different plasma sources has not been reported to date. In this paper, we investigate the Ru etch rate and the Ru to SiO_2 mask etch selectivity with varied process parameters, such as the gas flow ratio, the bias power, and the total gas flow rate and analyze the Ru

surface after the etching processes in both ICP and helicon etcher. Additionally, there are not many studies on the characteristics of Ru electrode etching at the pattern with a critical dimension (CD) of less than 0.20 μm. In this study, we report the etching characteristics of Ru electrodes with a CD of 0.15 μm using inductively coupled plasma (ICP) and helicon plasma.

2. Experimental details

Both patterned and blanket Ru wafers were used in our experiments. The pattern structure was substrate/TiN 500 Å/ Ru 4000 Å/TiN layer 600 Å/SiO_2 mask 3000 Å. SiO_2 mask, instead of photoresist mask, was used for patterning Ru, because oxygen gas was the main etchant in our experiments. The SiO_2 mask was patterned by $CF_4/N_2/Ar$ gas. The TiN layer was inserted between Ru and SiO_2 mask layer to prevent the cross-contamination of etching chamber. The TiN layer was patterned by Ar/Cl_2 gas. Since Ru cannot be etched by halogen gases only, due to high boiling point of their etch products, we used O_2 and Cl_2 gases, with the expectation that the volatile RuO_4 is produced [7,8].

We have used an ICP etcher and a helicon etcher for comparison. A DPS centura ICP tool commercially available from Applied Materials, Inc. and an $m=0$ helicon etcher

* Tel.: +82 32 860 7544; fax: +82 32 862 5546.
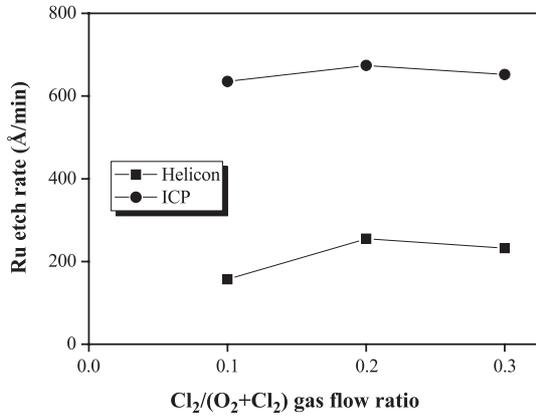 *E-mail address:* hwkim@inha.ac.kr.

Fig. 1. Variation of Ru etch rate with varying $Cl_2/(O_2+Cl_2)$ gas flow ratio.

commercially available from Trikon have been used. Helicon wave plasma sources were operated at the excitation frequencies of 13.56 MHz.

A scanning electron microscope (SEM) was used to measure the Ru etching rate and the Ru to SiO_2 etch selectivity. Ru surface after etching was analyzed by ex situ X-ray photoelectron spectroscopy (XPS) and transmission electron microscopy (TEM).

3. Results and discussion

In order to investigate the etching characteristics of Ru electrode using O_2/Cl_2 ICP and helicon plasma, we have varied the $Cl_2/(O_2+Cl_2)$ gas flow ratio and bias power. Fig. 1 shows the change of Ru etch rate with varying $Cl_2/(O_2+Cl_2)$ gas flow ratio ranging from 0.1 to 0.3 for typical etching conditions. For helicon plasma. the source power, bias power, total gas flow rate and pressure are set to 2000 W, 150 W, 50 sccm and 30 mTorr, respectively. For ICP, the source power, bias power, total gas flow rate and pressure are set to 1400 W, 200 W, 100 sccm and 20 mTorr, respectively. We reveal that the

higher etch rate is attained at the $Cl_2/(O_2+Cl_2)$ gas flow ratio of 0.2 than at the ratio of 0.1 and 0.3, regardless of plasma sources.

Fig. 2 shows the change of Ru etch rate and Ru to SiO_2 mask etch selectivity with varying bias power ranging from 100 to 300 W for typical etching conditions. For helicon plasma, the source power, total gas flow rate, $Cl_2/(O_2+Cl_2)$ gas flow ratio and pressure are set to 2000 W, 50 sccm, 0.2 and 30 mTorr, respectively. For ICP, the source power, total gas flow rate, $Cl_2/(O_2+Cl_2)$ gas flow ratio and pressure are set to 1400 W, 100 sccm, 0.2 and 20 mTorr, respectively. The Ru etch rate slightly changes with changing bias power in the range of 100–300W. However, the Ru to SiO_2 mask etch selectivity decreases considerably with increasing bias power due to the relatively significant increase of SiO_2 mask etch rate. As it is well known that SiO_2 etching is highly ion-controlled, the low variation of the Ru etch rate with bias power (e.g., the product of ion flux and ion energy) indicates that Ru etching for these plasma conditions does not dependent on the energetic ion flux.

In order to investigate the effect of total gas flow rate depending on the plasma sources, we set the pressure, bias power, source power, and $Cl_2/(O_2+Cl_2)$ gas flow ratio to be 20 mTorr, 200 W, 2000 W, and 0.2, respectively, for both plasma sources. Fig. 3 shows that Ru etch rate and Ru to SiO_2 mask etch selectivity increase with increasing total gas flow rate in the range of 100–300 sccm, regardless of plasma sources [10]. We surmise that the increased amount of etching species per unit time accelerates the Ru etching. It is noteworthy that the Ru etch rate using ICP is higher than that using helicon plasma at the etching condition with the same pressure, bias and source powers, and gas flow ratio. In order to study the difference caused by two plasma sources (observed in Fig. 3), we performed an XPS measurement. The samples were etched with the same process conditions with $Cl_2/(O_2+Cl_2)$ gas flow ratio of 0.2. We investigated the relative amounts of Ru, O, and Cl elements on the etched Ru surface below the depth of 100 Å, revealing that the relative amount of O element on the
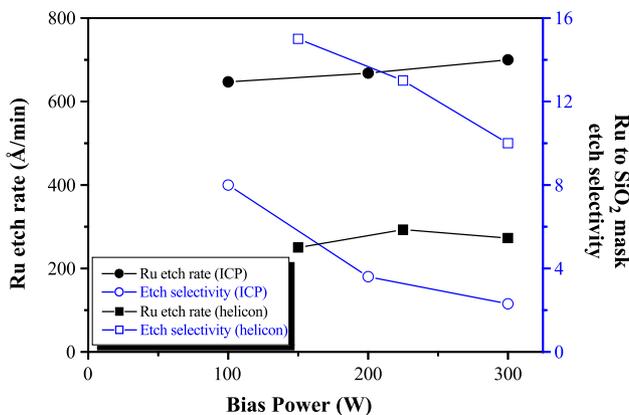

Fig. 2. Variation of Ru etch rate and Ru to SiO_2 mask etch selectivity with varying bias power.
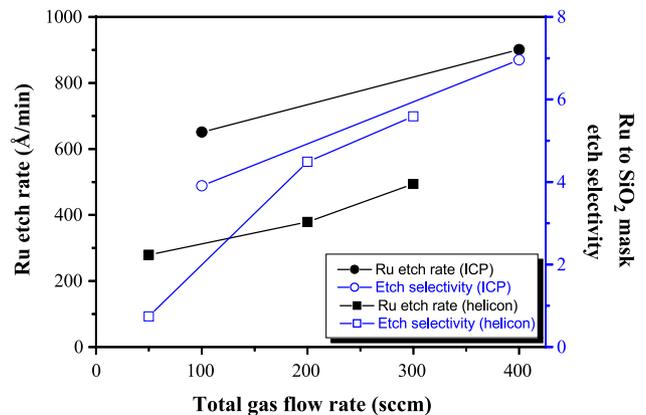

Fig. 3. Variation of Ru etch rate and Ru to SiO_2 mask etch selectivity with varying total gas flow rate.

Table 1
XPS measurement indicating the relative amounts of Ru, O, and Cl elements on the etched Ru surface below a depth of 100Å

Etcher	Ru (%)	O (%)	Cl (%)
Helicon	54.5	41.1	4.3
ICP	49.7	36.8	13.4

Ru surface etched using helicon plasma is greater than that using ICP (Table 1) [10]. On the other hand, the relative amount of Cl element on the Ru surface etched using helicon plasma is smaller than that using ICP.

We have compared TEM images of Ru etching profile using O_2/Cl_2 helicon plasma with those using O_2/Cl_2 ICP. The Ru etch rate of the sample using ICP is considerably higher than that when using helicon plasma. Fig. 4 shows a typical TEM image of a sample etched using O_2/Cl_2 helicon plasma with a Ru etch rate of about 250 Å/min, revealing that an additional layer is formed on top of the Ru layer. By obtaining the diffraction pattern, employing the Fourier transformation, and measuring the interlayer distance, we reveal that the additional layer consists of a mixture of amorphous and RuO_2 phases. The TEM image of a sample etched using O_2/Cl_2 ICP with a Ru etch rate of greater than 900 Å/min reveals that no additional layer is formed and the surface material is identified as pure Ru (not shown here).

The Ru etching may proceed by generation of RuO_2 from Ru, and subsequent generation of volatile RuO_4 from RuO_2. Since the Ru etch rate using ICP is higher than that using helicon plasma, we surmise that RuO_2 changes to RuO_4 more efficiently in case of ICP. In this case, we cannot observe the RuO_2 phase on the Ru surface. Since the result of Fig. 2 indicates that the Ru etching does not dependent on the energetic ion flux, we deduce that the radicals play a crucial role in Ru etching. We surmise that the ICP etcher generates radicals more efficiently, compared to the helicon etcher. Further study is necessary to
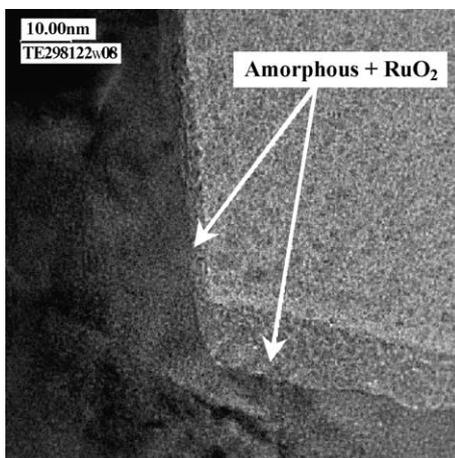

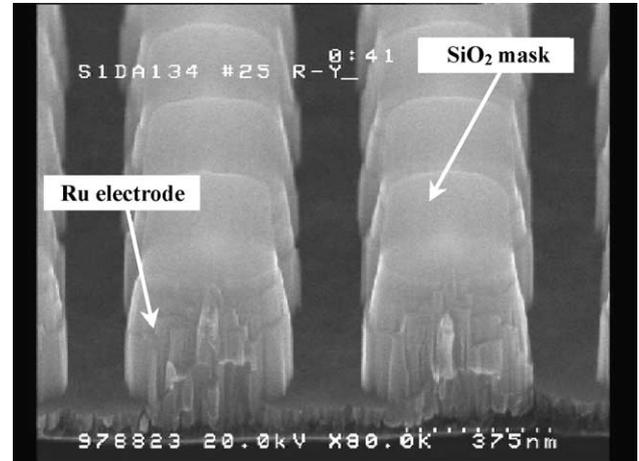Fig. 4. TEM image of Ru etching profile using O_2/Cl_2 helicon plasma.

Fig. 5. SEM image of Ru etching profile using ICP.

disclose the chemical nature of the radicals, which are mainly involved in the changing process of RuO_2 into the volatile RuO_4.

Fig. 5 shows the SEM images of patterned Ru electrode using O_2/Cl_2 ICP, cut along the long axis, revealing that an almost vertical etching slope of higher than 85° is obtained.

4. Conclusion

We have studied the etching of Ru electrode in ICP and helicon O_2/Cl_2 discharges. The Ru etch rate has its maximum value at the $Cl_2/(O_2+Cl_2)$ gas flow ratio in the range of 0.1–0.3 and increases with increasing the total gas flow rate, regardless of plasma sources. XPS reveals that the etched Ru surface using ICP with a high etch rate has a less amount of O element than that using helicon plasma with a low etch rate. TEM indicates that the Ru etched surface using ICP is pure Ru, while the etched Ru surface using helicon plasma is composed of amorphous and RuO_2. An etching slope of higher than 85° is obtained using ICP.

Acknowledgements

References

[1] H.W. Kim, B.S. Ju, B.Y. Nam, W.J. Yoo, C.J. Kang, T.H. Ahn, J.T. Moon, M.Y. Lee, J. Vac. Sci. Technol., A 17 (1999) 2151.

[2] T. Aoyama, S. Yamazaki, K. Imai, J. Electrochem. Soc. 145 (1998) 2961.

[3] W.J. Yoo, J.H. Hahm, H.W. Kim, C.O. Jung, Y.B. Koh, M.Y. Lee, Jpn. J. Appl. Phys. 35 (1995) 2501.

[4] K. Nishikama, Y. Kusumi, T. Oomori, M. Hanazaki, K. Namba, Jpn. J. Appl. Phys. 32 (1993) 6102.

[5] S. Yokoyama, Y. Ito, K. Ishihara, K. Hamada, S. Ohnishi, J. Kudo, K. Sakiyama, Jpn. J. Appl. Phys. 34 (1995) 767.

[6] H.W. Kim, B.S. Ju, C.J. Kang, J.T. Moon, Microelectron. Eng. 65 (2003) 185.

[7] S. Saito, K. Kuramasu, Jpn. J. Appl. Phys. 31 (1992) 135.

[8] W. Pan, S.B. Desu, J. Vac. Sci. Technol., B 12 (1994) 3208.

[9] W.E. Bell, M. Tagami, J. Phys. Chem. 67 (1963) 2433.

[10] H.W. Kim, J.-H. Han, B.-S. Ju, C.-J. Kang, J.-T. Moon, Mater. Sci. Eng., B 95 (2002) 249.